

Abstract

A common approach to measuring many cellular processes by image analysis is to start with segmenting the image into compartments of interest. Vitro Bioscience has developed a method of analysis of cytoplasm to nucleus translocation (CNT) that does not require subcellular segmentation. It can be performed individually on a cell-by-cell basis or globally on the whole image. The method is based on modeling and analysis of the 2D distributions of stains: signal (i.e. protein stain) and nuclear counterstain. The method does not have any user parameters and is very tolerant to variation in image acquisition. We analyzed the performance of this new method with respect to cell type, magnification, number of analyzed cells, accuracy of focusing, depth of field, and plate flatness. Using statistical methods to measure the quality of data produced by this new algorithm, we confirmed that it performs better than our implementation of algorithms based on segmentation. The performance assessment methodology will be discussed in the context of Vitro's application of this algorithm to measure translocation events at varying magnifications on the CellCard™ System and in the future on CellPlex™ assays. Furthermore, the presented performance assessment methodology can be used in the future to design the best screening strategy and to compare different cell analysis algorithms.

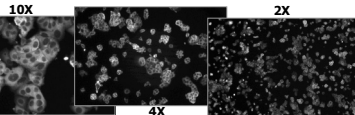
Experiment design

| Cell | 1 | 2 | 3 | 4 | 5 | 6 | 7 | 8 | 9 | 10 | 11 | 12 | 13 | 14 | 15 |
|------|------|------|------|------|------|------|------|------|------|------|------|------|------|------|------|
| A | 0.78 | 0.82 | 0.85 | 0.88 | 0.92 | 0.95 | 0.98 | 1.02 | 1.05 | 1.08 | 1.12 | 1.15 | 1.18 | 1.22 | 1.25 |
| B | 0.75 | 0.78 | 0.82 | 0.85 | 0.88 | 0.92 | 0.95 | 0.98 | 1.02 | 1.05 | 1.08 | 1.12 | 1.15 | 1.18 | 1.22 |
| C | 0.72 | 0.75 | 0.78 | 0.82 | 0.85 | 0.88 | 0.92 | 0.95 | 0.98 | 1.02 | 1.05 | 1.08 | 1.12 | 1.15 | 1.18 |
| D | 0.70 | 0.72 | 0.75 | 0.78 | 0.82 | 0.85 | 0.88 | 0.92 | 0.95 | 0.98 | 1.02 | 1.05 | 1.08 | 1.12 | 1.15 |
| E | 0.68 | 0.70 | 0.72 | 0.75 | 0.78 | 0.82 | 0.85 | 0.88 | 0.92 | 0.95 | 0.98 | 1.02 | 1.05 | 1.08 | 1.12 |
| F | 0.65 | 0.68 | 0.70 | 0.72 | 0.75 | 0.78 | 0.82 | 0.85 | 0.88 | 0.92 | 0.95 | 0.98 | 1.02 | 1.05 | 1.08 |

CellCard™ MCF7 A549 TNF-concentration in ng/ml

Cells were plated at about 10,000 cells per well in a 96 well microtiter plate (Packard ViewPlate) and incubated overnight. The cells were then treated with varying doses of TNF α , up to 100nm, for 30 minutes. This treatment results in the activation of NF κ B and the translocation of the p65 subunit from the cytoplasm to the nucleus. The cells were subsequently fixed and immuno-stained for p65 and counterstained with the Hoechst nuclear dye.

The plate was scanned three times at 10X, 4X, and 2X magnifications acquiring one image per well and analyzed with the Vitro Bioscience algorithm. The data was then plotted and analyzed for quality using the V and Z factor calculations.



Images and profiles of model and real cells

To find a robust measure of nuclear translocation we have defined a model of spatial distribution of the nuclear counterstain and of the signal stain as it moves from the cytoplasm to the nucleus. The model was studied under some perturbations in order to find measures that are robust. The model of cell staining comprises a bell-shaped intensity distribution of counterstain, shown in blue, and a bell-shaped distribution of signal stain shown in green.

A, B – profiles through model distributions; C, D – profiles through real cells. A, C – negative, B, D – positive. Blue – counterstain, green – signal stain.

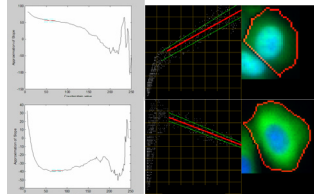
For the negative case the distribution of signal stain is wider and has a bell-shaped crater. Profiles through the real cells show substantial similarity to the model profiles. (Profile C is plotted through two cells, profile D – through three cells. All profiles are independently normalized to their intensity maxima.)

Model and experimental 2D distributions

To derive stable measures that characterize transitions from the negative to the positive case, we analyzed joint distributions of the stains on the model and on real cells. In the ideal case, the model spatial stain distributions are circularly symmetrical and aligned. The cross-histogram for this case is shown in panels A and B. If the model is perturbed by offsetting the centers of the two stains, by changing shape from circular to oval, or by adding noise, the distributions become fuzzy as shown in panels C and D. Typical negative and positive real cells have cross-histogram as shown in panels E and F. These distributions suggest that a translocation measure can be defined as the slope of a straight-line segment approximating the right side of the cross-histogram.

This portion of the distribution corresponds to the more intense nuclear staining and is also close to the center of the nucleus. The farther from the center, the more diffuse the distribution, and the less reliable the approximation becomes.

Parameters derived from 2D distributions



The portion of the distribution that is used for approximation with the straight line is found by plotting the approximated slope going from right to left and selecting the range where this approximation is the most stable. Color lines show the resulting value of slope. Top panel – nuclear localization (positive), bottom panel – cytoplasm localization (negative) of protein.

A variation on this method is to calculate two more slopes as shown in panels on the right. The top line is the regression line calculated on all points above the original slope segment (which we will refer to as Slope1); the bottom line is the regression line calculated on all points below the original slope segment. If all three slopes have the same sign, the result is the one with the greatest absolute value. If they have different signs, then the original slope is chosen. We call this measure Slope2.

The described method can be applied globally to the whole image, and to a cluster of cells. Application of the method on the individual cell level neutralizes variation in expression or staining, which in the case of translocation may be non-informative. In some cases (e.g., low magnification) partitioning the image into individual cells is difficult; then the analysis can be done on clusters of closely situated cells. The variation among cells or clusters can be due also to technical reasons, e.g. illumination nonuniformity. To apply the analysis to individual cells, there is no need to know the cell or nuclear boundary. All that is needed is to know the area within which a separate cell is contained.

Partitioning into components - markers

Partitioning into components serves a dual purpose. The first is for individual cell analysis; the second – as a step in optional intensity equalization. There are two main steps in the partitioning method: finding of markers and finding of separation lines. Markers are found by the following algorithm. A fixed value (marker contrast) is subtracted with saturation from the image of nuclear counterstain and the resulting image is reconstructed within the image of nuclear counterstain. This image is then subtracted from the counterstain image and the result is converted to binary image. The components of this image are the markers. A further restriction may be imposed on markers – only markers that have at least one pixel above a given threshold (marker brightness) are retained for the second step. Depending on magnification and noise level the image of nuclear counterstain may be smoothed prior to this algorithm. This method of determining markers can handle cells of different size and shape. Other methods, e.g. based on top-hat transform may be used too.

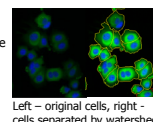
Partitioning into components - watersheds of combined intensity images

Separation lines are defined as the watershed of the inverted image of the linear combination of the counterstain image and the signal stain image. The reason to use linear combination rather than just the nuclear counterstain image is that cells are often nonsymmetrical and unevenly shaped. Separation lines from nuclear stain image may cut through the middle of cells. The use of signal stain produces more accurate separation lines. Coefficients of linear combination for the nuclear image = 0.3, for the signal stain = 0.7

Left – image partitioning using only nuclear stain image (blue). Right – image partitioning using linear combination of nuclear and signal stains. Coefficient of linear combination for the nuclear image = 0.3, for the signal stain = 0.7

Normalization of intensities

The joint distributions of counterstain and signal stain are normalized to their respective maxima. This can be done for the distribution or for the image. The result is the same but normalizing the image gives additional feedback to the user and may reveal features that were not seen before normalization.

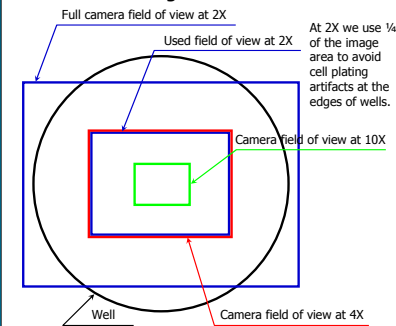


Left – original cells, right – cells separated by watershed lines with intensities of the counterstain (blue) and signal stain (green) normalized to the maximum in each compartment.

Normalization can be done in components described above. In this case all pixels from a component are multiplied by the same number, separately for signal stain and for counterstain.

Alternatively, normalization can be done without partitioning the image by fitting a smooth surface to the images of signal stain and counterstain.

Image acquisition - fields of view at different magnifications

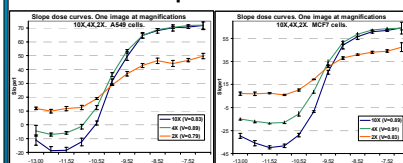


V-factor – a measure of assay quality

To measure assay quality (or in a more narrow sense, algorithm quality) we use V-factor¹, given by the formula below. It generalizes Z-factor for a dose-dependent sequence by assay states and gives a more realistic measure of the overall assay performance by accounting for intermediate points in the dose curve, which have higher variability due to effects of competition and of dispensing errors. The numerical representation was chosen so that V-factor reverts to Z-factor if there are only two states-positive and negative.

$$V = 1 - 6 \left(\frac{\text{Average } SD}{|M_{pos} - M_{neg}|} \right)$$

Dynamic range and V-factor at one image per well



At lower magnifications the dynamic range is reduced, but the variability is also reduced, so the quality (V-factor) remains about the same. This may be due to the greater number of cells in one image at lower magnifications.

Comparison of slope and mask (N2R) algorithms at 10X. Parameter dependency of the mask algorithm.

| A549 | | | | | | | | | | | |
|--------|------|------|------|----------------|------|------|------|--------------------------|------|------|------|
| Slope1 | | | | Slope1 alcohol | | | | Slope1 nuclear erosion=1 | | | |
| N2R | | | | N2R | | | | N2R | | | |
| Gap | 1 | 2 | 3 | 4 | 5 | 6 | 7 | 8 | 9 | 10 | 11 |
| 0 | 0.97 | 0.81 | 0.81 | 0.80 | 0.80 | 0.80 | 0.80 | 0.80 | 0.80 | 0.80 | 0.80 |
| 1 | 0.81 | 0.80 | 0.80 | 0.80 | 0.80 | 0.80 | 0.80 | 0.80 | 0.80 | 0.80 | 0.80 |
| 2 | 0.79 | 0.78 | 0.78 | 0.79 | 0.80 | 0.80 | 0.80 | 0.80 | 0.80 | 0.80 | 0.80 |
| 3 | 0.78 | 0.78 | 0.78 | 0.80 | 0.81 | 0.81 | 0.81 | 0.81 | 0.81 | 0.81 | 0.81 |
| 4 | 0.79 | 0.79 | 0.80 | 0.81 | 0.82 | 0.82 | 0.82 | 0.82 | 0.82 | 0.82 | 0.82 |

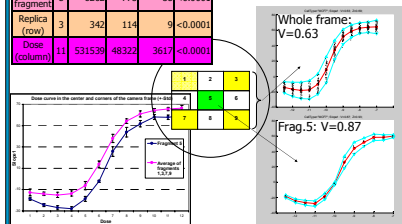
- The mask-based algorithm shows significant dependency of quality on parameters. The slope algorithm has no parameters.
- The slope algorithm gives better quality than mask-based algorithm at any parameter setting.
- The slope algorithm applied globally is almost as good as when applied on a cell-by-cell basis and is faster to compute.

Assay quality and well flatness

Example: Slope1 for MCF7 cells at 4X

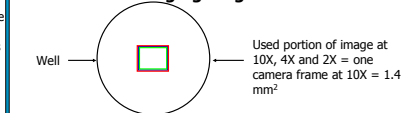
| V-factor | 0.91 | 0.76 | 0.63 | 0.56 | 0.51 | 0.48 |
|-----------------|------|------|------|------|------|------|
| Number of cells | 4300 | 1100 | 500 | 290 | 190 | 130 |

Is the increased variability due only to the smaller numbers of cells, or are there other factors?



Due to non-flat well bottom the center and periphery of the image are in different focal positions. This leads to the shift of the dose curve and increased variation. Using subset of the image gives better quality than the whole image.

Assay quality at different number of cells and imaging magnification



| | | MCF7 | | | Magnification | | |
|----------------------------|--------------------|-----------------|------|------|---------------|--|--|
| Required CellCard carriers | Image size (sq.mm) | Number of cells | 2X | 4X | 10X | | |
| 14 | 1.40 | ~700 | 0.78 | 0.87 | 0.89 | | |
| 3-4 | 0.35 | ~180 | 0.58 | 0.65 | 0.66 | | |
| 1-2 | 0.16 | ~80 | 0.43 | 0.55 | 0.59 | | |

| | | A549 | | | Magnification | | |
|----------------------------|--------------------|-----------------|------|------|---------------|--|--|
| Required CellCard carriers | Image size (sq.mm) | Number of cells | 2X | 4X | 10X | | |
| 14 | 1.40 | ~500 | 0.74 | 0.83 | 0.83 | | |
| 3-4 | 0.35 | ~130 | 0.58 | 0.65 | 0.66 | | |
| 1-2 | 0.16 | ~60 | 0.36 | 0.58 | 0.59 | | |

Conclusions

- A new method for the analysis of cytoplasm to nucleus translocation images is presented; it does not have user parameters and provides superior quality of data compared with mask-based method.
- Segmentation of intracellular compartments may not be necessary for quantitation of intracellular processes.
- V-factor proved to be a useful benchmark to compare image analysis algorithms/measures and to determine image resolution and image size/cell number requirements.
- Better assay design and analysis can be achieved by using presented methodologies for the analysis of dependency of assay measures on cell type, magnification, number of analyzed cells, accuracy of focusing, depth of field, pixel shift and plate flatness.
- Less is more: choosing a subset of cells in the same focal plane may improve assay quality; alternatively, increasing the cell number only helps if all cells are in focus.
- The cell number and magnification requirements of cytoplasm to nucleus translocation assay put it within the parameter range of the CellCard system.
- Future developments of this algorithm will focus on enabling CellPlex assays on the CellCard System.

References

- I. Ravkin "Quality Measures for Imaging-based Cellular Assays" SBB 2004 conference poster #P12024.